Evolution of magmatic and subsolidus AFM mineral assemblages in granitoid rocks: Biotite, muscovite, and garnet in the Cuffytown Creek pluton, South Carolina

J. Alexander Speer

Department of Marine, Earth, and Atmospheric Sciences, Box 8208, North Carolina State University, Raleigh, North Carolina 27695-8208, U.S.A.

Susan W. Becker

101 Yeonas Circle SE, Vienna, Virginia 22180, U.S.A.

Abstract

The Cuffytown Creek pluton is a leucocratic alkali feldspar granite with (F + Mn)-rich biotite, muscovite, garnet, and fluorite as varietal minerals. Bt ± Ms is preserved as inclusion assemblages in quartz; Bt + Ms ± Grt and Ms + Grt are matrix assemblages. The inclusion assemblages are interpreted as early magmatic, and the matrix assemblages as late magmatic with superimposed subsolidus partial reequilibration. In sequence, the AFMMn crystallization reactions are liquid = Bt, liquid = Bt + Ms, liquid + Bt = Ms + Grt, and liquid = Grt + Ms. Inclusion biotite shows $FeMg_{-1}$ and $Mn(Fe,Mg)_{-1}$ exchanges, which may reflect both change in melt composition and cooling along an f_{O_2} buffer. Inclusions of white mica are nearly end-member muscovite. Evolution from inclusion to matrix mica compositions shows narrowing of the compositional gap between the dioctahedral and trioctahedral micas, as well as OHF_{-1} and $MnMg_{-1}$ exchanges in the biotite and $(Fe^{2+},Mg,Mn)Si^{[6]}Al_{-1}^{[4]}Al_{-1}$ (celadonite), NaK_{-1}, OHF_{-1}, and Ti enrichment in the white micas. Garnets are spessartine-almandine.

The liquid line of descent indicates that the melt became increasingly rich in Fe/(Fe + Mg) and Mn/(Fe + Mn) with decreasing temperatures, but each at differing rates at differing stages during crystallization. Peraluminosity of the melt increased rapidly at first, then decreased slightly before increasing at a much slower rate. Final crystallization conditions are estimated at 650 °C and 2–3 kbar. Miarolitic cavities indicate that, at the end of crystallization, $P_{fluid} = P_{tot}$, and a separate fluid phase formed that persisted into the subsolidus. The fluid was dominantly H_2O, with lesser amounts of F [$\log(f_{H_2O}/f_{HF}) = 3.16$–3.54].

Subsolidus replacement textures, mineral compositions, and fluid buffers result from two reactions that are estimated to have occurred at 300–400 °C: (1) plagioclase + iron biotite + muscovite + iron chlorite + fluid = albite + potassium feldspar + magnesium biotite + phengite + magnesium chlorite + fluorite + quartz and (2) garnet + potassium feldspar + fluid = muscovite + rhodochrosite + quartz.

Introduction

Investigating sequences of magmatic AFM mineral crystallization reactions in granites is difficult because, among other reasons, we are forced to rely on observations from different samples or even differing rock types of composite plutons. We must interpret the relationships among the samples or rock types and assume that they represent parts of a continuous liquid line of descent. Individual samples from the Cuffytown Creek, South Carolina, pluton contain two texturally distinct AFMMn assemblages: biotite ± muscovite assemblages included in quartz and muscovite + garnet ± biotite matrix assemblages. We investigate these assemblages as a sequence of magmatic or subsolidus crystallization reactions that evolved within the same rock volume. Because the Cuffytown Creek pluton is an evolved granite, its mineral

relations should also provide some insight into the final liquidus AFMMn crystallization reactions of granites involving biotite, muscovite, and garnet and discussed with varying amounts of agreement by Miller and Stoddard (1980, 1981), Abbott (1981a, 1981b, 1985), and Zen (1988).

Geologic setting

The Cuffytown Creek pluton, which is 293 ± 14 m.y. old, is exposed in an oval-shaped area of 20 km² in the Carolina slate belt of Edgefield and McCormick Counties, South Carolina (Fig. 1). Speer and Becker (1990) described the geology, petrography, and geochemistry of the Cuffytown Creek, as well as the previous work on it; the description here is a summary of that work.

The pluton comprises unfoliated, leucocratic, medium-
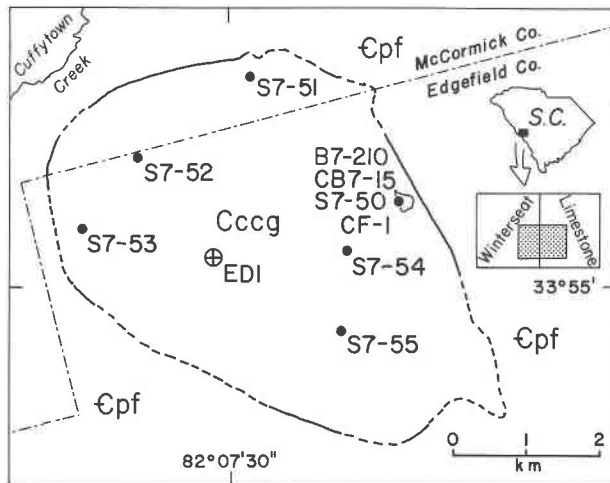
Fig. 1. Geologic and sample map of the Cuffytown Creek pluton, South Carolina (after Speer and Becker, 1990). Cccg = Carboniferous Cuffytown Creek granite, Cpf = Cambrian Persimmon Fork formation, ED1 = drill core.

grained alkali-feldspar granite, with a color index between 2.2 and 5.3 and scarce phenocrysts of quartz and alkali feldspar up to 2 cm in length. Pegmatite and aplite veins are rare. Varietal minerals are (F + Mn)-rich biotite, F-rich white mica, F-bearing spessartine-almandine garnet, chlorite, and fluorite. Accessory minerals include allanite, apatite, carbonate, fergusonite, hematite, ilmenite, magnetite, manganocolumbite, monazite, pyrite, niobian rutile, sphalerite, titanite, xenotime, and zircon. Bismuth lead and bismuth tellurium sulfides (cosalite and tetradymite?) occur in veins.

Major- and trace-element analyses show the Cuffytown Creek granite to be low in Al, Ti, Ca, Mg, Ba, and Sr and high in Si, Fe/Mg, F, Ga, Nb, Rb, Th, Y, and U, as

compared with calc-alkaline granitoids. Rock compositions lie at the metaluminous-peraluminous boundary, normative Q + Or + Ab = 95–98% and Rb/Sr = 45. A large gravity low is centered on the pluton, and we conclude that the surface exposure is only the top of a much larger body and that it crystallized from a highly fractionated, felsic melt in the cupola of a magma chamber.

The Cuffytown Creek pluton is emplaced in greenschist-grade metavolcanics of the Persimmon Fork Formation of late Precambrian(?) to Cambrian in age in the Carolina slate belt. The wall rocks were metamorphosed to the low-pressure amphibolite facies, with assemblages containing hornblende, andesine, and clinopyroxene. Locally, there are skarns containing abundant quartz and fluorite, with epidote, andradite, and manganiferous hedenbergite.

MINERAL RELATIONS

Compositions of the minerals in polished thin sections were determined on a nine-spectrometer ARL-SEMQ (Virginia Polytechnic Institute), using the analytical scheme described by Solberg and Speer (1982), and a Cameca Camebax SX 50 (University of South Carolina). Analyses are reported in Appendix 1,[1] and selected analyses given in Tables 1–4. Mineral abbreviations in the text, tables, and figures are those recommended by the *American Mineralogist* (Kretz, 1983). Color designations are those of the Rock-Color Chart Committee (1980).

Feldspars

Macro- to microperthitic alkali feldspar exhibits both primary Carlsbad growth twins and microcline albite-

TABLE 1.   Selected biotite analyses for the Cuffytown Creek pluton, South Carolina

	1	2	3	4	5	6	7	8	9	10
SiO_2	38.84	38.07	38.42	38.39	37.86	37.42	39.18	39.24	38.07	38.52
TiO_2	2.08	1.68	1.64	1.61	1.21	1.66	1.59	1.24	1.72	1.70
Al_2O_3	12.76	18.53	18.62	18.22	12.99	16.57	18.90	12.76	13.62	17.59
FeO*	18.80	18.58	18.74	18.30	18.68	18.66	19.00	14.75	18.44	18.28
MnO	2.23	3.37	4.32	2.19	3.03	2.87	4.41	1.77	2.64	3.66
MgO	12.53	4.89	4.15	5.98	10.66	4.85	4.22	13.89	9.83	5.96
CaO	0.14	0.01	0.0	0.03	0.14	0.14	0.0	0.14	0.14	0.0
Na_2O	0.27	0.08	0.09	0.12	0.25	0.21	0.08	0.18	0.20	0.14
K_2O	9.87	9.98	9.86	9.83	9.51	9.44	9.05	9.77	9.70	9.01
BaO	0.23	—	—	—	0.21	0.21	—	0.21	0.20	—
F	3.97	—	—	—	4.18	2.72	—	4.26	4.11	—
Cl	0.10	—	—	—	0.10	0.05	—	0.08	0.07	—
H_2O**	2.09	3.89	3.92	3.92	1.84	2.47	3.98	1.89	1.90	3.92
−O = F + Cl	1.69	—	—	—	1.78	1.16	—	1.81	1.75	—
Total	102.22	99.00	99.76	98.59	98.88	96.11	100.86	98.37	98.89	98.78

Note: (1) CB7-15 = biotite included in quartz. (2) CB7-15 = average of eight matrix-biotite analyses. (3) S7-50a = biotite included in quartz. (4) S7-50a = average of seven analyses, inclusion biotite reequilibrated with the matrix. (5) S7-55 = average of four biotite samples included in quartz analyses. (6) S7-55 = matrix biotite with muscovite. (7) ED1-872 = average of three analyses, inclusion biotite reequilibrated with the matrix. (8) ED1-877 = biotite included in quartz. (9) ED1-877 = biotite included in quartz. (10) ED1-926 = average of three biotite samples included in quartz analyses.
 * All Fe reported as FeO.
 ** Calculated on the basis of (OH + F + Cl) = 2/24 anions.

TABLE 2. Selected white mica analyses for the Cuffytown Creek pluton, South Carolina

	1	2	3	4	5	6	7	8	9	10
SiO_2	47.11	47.27	48.83	45.84	46.50	45.82	46.35	46.13	45.01	49.42
TiO_2	0.10	0.28	0.55	0.17	0.59	0.71	0.43	0.13	0.58	0.64
Al_2O_3	32.81	27.48	30.31	35.86	27.11	26.33	30.70	34.95	27.49	29.05
FeO*	4.00	6.03	6.48	1.50	6.76	7.35	5.01	2.40	7.18	7.85
MnO	0.76	1.09	0.76	0.54	0.70	1.18	0.71	0.60	1.00	1.11
MgO	0.37	1.72	2.08	0.03	2.41	2.14	0.67	0.05	1.84	2.03
CaO	0.12	0.14	0.0	0.03	0.01	0.12	0.13	0.0	0.08	0.0
Na_2O	0.41	0.43	0.22	0.49	0.27	0.42	0.31	0.50	0.39	0.20
K_2O	9.71	8.74	7.88	10.37	10.87	8.79	9.40	10.34	9.50	6.83
BaO	0.21	0.19	—	—	—	0.19	0.18	—	—	—
F	0.73	1.23	—	0.54	1.14	1.96	0.97	0.42	1.18	—
Cl	0.03	0.03	—	0.02	0.02	0.04	0.04	0.01	0.01	—
H_2O^{**}	4.10	3.72	4.53	4.21	3.79	3.31	3.89	4.27	3.68	4.53
$-O = F + Cl$	0.31	0.52	—	0.23	0.48	0.83	0.42	0.18	0.50	—
Total	100.15	97.83	101.64	99.37	99.69	97.53	98.37	99.64	97.44	101.66

Note: (1) CB7-15 = muscovite in plagioclase. (2) CB7-15 = white matrix mica. (3) S7-50a = average of six white matrix-mica analyses. (4) S7-53 = average of three muscovite included in quartz analyses. (5) S7-53 = white matrix mica. (6) S7-55 = average of four white matrix-mica analyses. (7) ED1-877 = average of four white matrix-mica analyses. (8) ED1-834 = average of four muscovite included in quartz analyses. (9) ED1-834 = white matrix mica. (10) ED1-926 = muscovite with chlorite, pseudomorph after magnetite.
* All Fe reported as FeO.
** Calculated on the basis of (OH + F + Cl) = 2/24 anions.

pericline twins. Plagioclase forms white to very light gray grains, twinned according to the albite and pericline laws. Most feldspar is subhedral, but it is locally euhedral in miarolitic cavities. Also feldspar is euhedral when found with muscovite, fluorite, and carbonate minerals in what we interpret as filled cavities. Both alkali and plagioclase feldspars have local overgrowths of clear albite in these vugs.

Broad-beam microprobe analyses (Appendix 1) give an estimated original bulk alkali feldspar composition of $An_0Ab_{8.8}Or_{91.1}$. Point microprobe analyses show that exsolved albite is $An_{0.7-1.6}Ab_{97.3-98.7}Or_{0.6-1.1}$; exsolved potassic feldspar is $An_{0-0.3}Ab_{1.8-4.9}Or_{95.2-98.2}$. Plagioclase has compositions of $An_{0.6}–An_{8.9}$; potassium contents of the plagioclase are $Or_{0.8}–Or_{2.3}$, with an average of $Or_{1.2}$ (Appendix 1).

Biotite

Brownish black biotite makes up less than 1 modal% of the Cuffytown Creek granites and is absent from several samples. It forms pleochroic (moderate olive brown to grayish yellow) flakes or shreds up to 3 mm long. Most biotite occurs as anhedral grains, interstitial to feldspars and quartz, and most of these matrix grains are partially altered and interleaved with white mica and chlorite (Fig. 2a). Small, subhedral, unaltered biotite, isolated from the groundmass, occurs as scarce inclusions in quartz (Fig. 2b) and, rarely, with white mica (Fig. 2c).

Microprobe analyses show that the Cuffytown Creek biotite falls approximately midway between phlogopite and annite (Appendix 1, Table 1). The biotite is much less aluminous than biotite in other late Paleozoic granites of the southern Appalachians (Fig. 3). Matrix biotite

TABLE 3. Selected garnet analyses for the Cuffytown Creek pluton, South Carolina

	1	2	3	4	5	6
SiO_2	35.97	36.50	36.14	35.00	34.06	33.93
TiO_2	0.30	0.0	0.23	0.33	0.10	0.10
Al_2O_3	20.65	21.86	20.63	19.94	19.83	19.91
FeO*	11.56	13.63	12.95	9.94	10.26	9.59
MnO	31.49	29.65	29.85	32.76	33.06	33.61
MgO	0.22	0.15	0.39	0.41	0.60	0.71
CaO	0.61	0.52	0.66	0.96	0.13	0.11
F	—	—	0.43	0.92	—	—
$-O = F$	—	—	0.18	0.38	—	—
Total	100.80	102.31	101.10	99.88	98.04	97.96
			Garnet components			
Alm	25.09	30.56	27.44	18.33	20.21	18.63
Prp	0.89	0.60	1.58	1.71	2.45	2.90
Sps	72.24	67.34	69.04	77.11	76.95	78.15
Grs	1.78	1.49	1.95	2.84	0.39	0.32

Note: (1) CB7-15C = garnet core. (2) CB7-15 = garnet rim. (3) CB7-15 = garnet with F determination. (4) S7-55 = average of four analyses, garnet with F determinations. (5) ED1-872 = garnet core. (6) ED1-872 = garnet rim.
* All Fe reported as FeO.

TABLE 4. Selected chlorite analyses for the Cuffytown Creek pluton, South Carolina

	1	2	3	4	5	6
SiO_2	23.60	24.71	24.05	23.88	22.41	27.44
TiO_2	0.0	0.10	0.03	0.02	0.0	0.07
Al_2O_3	17.98	19.81	21.86	18.94	19.69	20.40
FeO*	43.65	37.29	37.99	40.99	44.53	37.65
MnO	0.87	0.53	0.59	1.13	0.46	0.36
MgO	2.20	4.90	2.07	2.88	0.33	0.18
CaO	0.01	0.01	0.01	0.02	0.0	0.09
Na_2O	0.01	0.01	0.03	0.02	0.0	0.08
K_2O	0.0	0.05	0.02	0.0	0.01	1.93
H_2O^{**}	10.23	10.58	10.46	10.34	10.08	10.66
Total	98.55	97.99	97.11	98.22	97.51	98.86

Note: (1) S7-50a = average of two analyses, chlorite intergrown with muscovite. (2) S7-53 = average of two analyses, chlorite intergrown with muscovite. (3) S7-55 = average of two analyses, chlorite intergrown with muscovite. (4) ED1-872 = average of three analyses. (5) ED1-926 = chlorite with muscovite, pseudomorph after magnetite. (6) ED1-926 = chlorite intergrown with biotite and muscovite.
* All Fe reported as FeO.
** Calculated on the basis of (OH + F + Cl) = 16/36 anions.
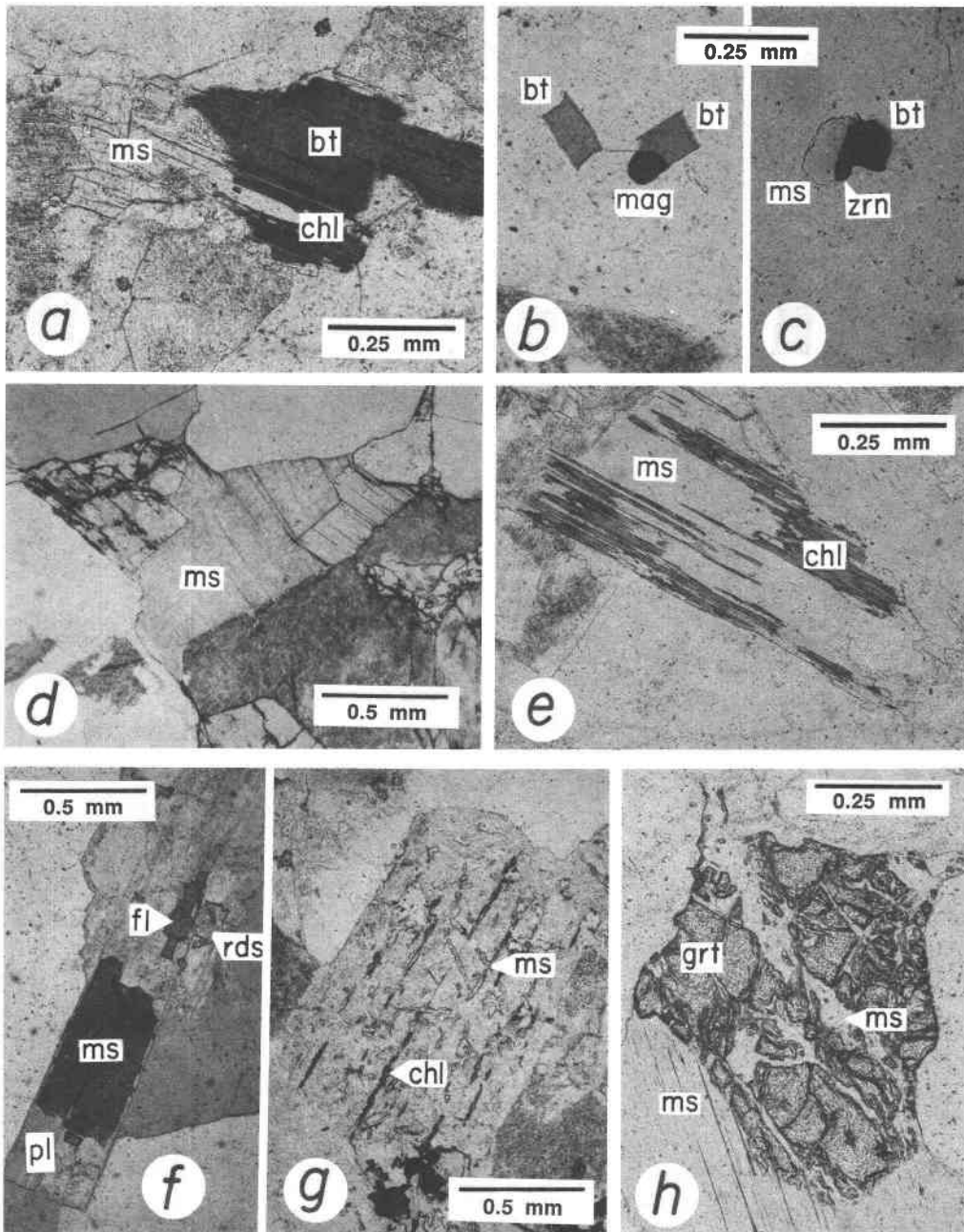
Fig. 2.   Photomicrographs of mica textures. (**a**) Matrix biotite (bt) partially replaced with white mica (ms) and chlorite (chl) and minor hematite + rutile ± fluorite (B7-211). (**b**) Anhedral biotite and magnetite (mag) included in quartz and interpreted as the earliest generation of biotite preserved in the Cuffytown Creek granite (ED1-877.5). (**c**) Inclusion biotite + white mica assemblage with zircon (zrn) in quartz (S7-53). (**d**) White matrix mica interstitial to euhedral feldspars (S7-50d). (**e**) Interleaved white mica + chlorite interpreted as replacements or pseudomorphs of biotite (CB7-15). (**f**) Single large grain of white mica replacing plagioclase (ED1-917.5). Also replacing the plagioclase are fluorite (fl) and carbonate (rds). (**g**) Oriented white mica and chlorite replacements of plagioclase (B7-210c). (**h**) Garnet (grt) partially replaced by the adjacent, large matrix white mica and fine-grained white mica along fractures (ED1-917.5).

is more Fe rich [$Fe/(Fe + Mg) = 0.61–0.75$] than inclusion biotite [$Fe/(Fe + Mg) = 0.37–0.54$] (Fig. 3). The few inclusion biotite samples with $Fe/(Fe + Mg)$ compositions similar to the matrix biotite samples are considered to have equilibrated with the minerals outside the quartz grain by the now-healed fractures and are grouped with matrix biotite in all subsequent diagrams and discussions.
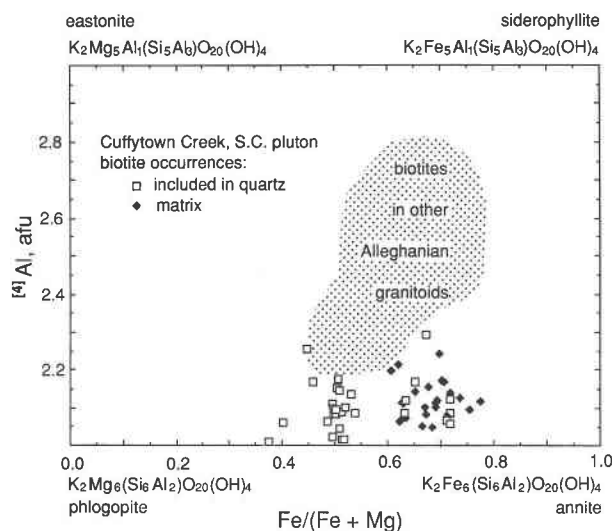
Fig. 3. Compositions of biotite from the Cuffytown Creek pluton projected onto the phlogopite-annite-eastonite-siderophyllite field and differentiated by occurrence. Field of biotite compositions from other Alleghanian granites from the southern Appalachians is from Speer et al. (1980); Speer (1981, 1982, 1987); Russell et al. (1985); and Speer et al. (1986).

In addition to being Fe rich, matrix biotite has greater octahedral Al (average of 1.19 vs. 0.33 afu), lower Mg (average of 1.11 vs. 2.50 afu), a wider and higher range of Mn (average of 0.44 vs. 0.32 afu), and lower F (2.7–3.0 wt% vs. 4.0–4.3 wt% F) than the inclusion biotite (Figs. 4a–4c). Both matrix and inclusion biotite have nearly full interlayer K occupancy (Fig. 4d), similar titania contents (averages of 0.19 vs. 0.17 afu), and little Cl (<0.034 afu).

Inclusion biotite shows an $FeMg_{-1}$ exchange responsible for the range in Fe/(Fe + Mg), whereas the variation of Fe/(Fe + Mg) in matrix biotite results from differences in Mg while Fe remains more or less constant (Fig. 4b). Constant [4]Al with decreasing Mg (Fig. 3) rules out an $^{[4]}Al^{[6]}AlMg_{-1}Si_{-1}$ (Al-Tschermak) substitution. On the basis of the variation in [6]Al (Fig. 4a), we conclude that Fe becomes oxidized, and that the exchange vector relating the compositions of the matrix biotite is $^{[6]}AlFe^{3+[6]}_{-1}\square Fe^{2+}_{-1}Mg_{-2}$. This is a dioctahedral-trioctahedral mica substitution: matrix biotite has a significant dioctahedral mica content, whereas inclusion biotite is a nearly trioctahedral end-member (Fig. 5). The nearly K-filled interlayer (Fig. 4d) precludes the possibility that the increasing [6]Al content in the biotite results from alteration to chlorite or kaolinite.

Either a zinnwaldite, $^{[6]}Al^{[6]}LiMg_{-2}$, or lepidolite, $Si^{[6]}Li^{[4]}Al_{-1}Mg_{-1}$, substitution could explain the Mg variation without a change in the Fe content of the matrix biotite. Li substitution could also explain an apparent dioctahedral content of the matrix biotite (Monier and Robert, 1986c). Lack of any systematic variation in the tetrahedral-site composition as a function of Mg content rules out lepidolite substitution. However, decreasing Mg at constant Fe in the matrix biotite could be explained
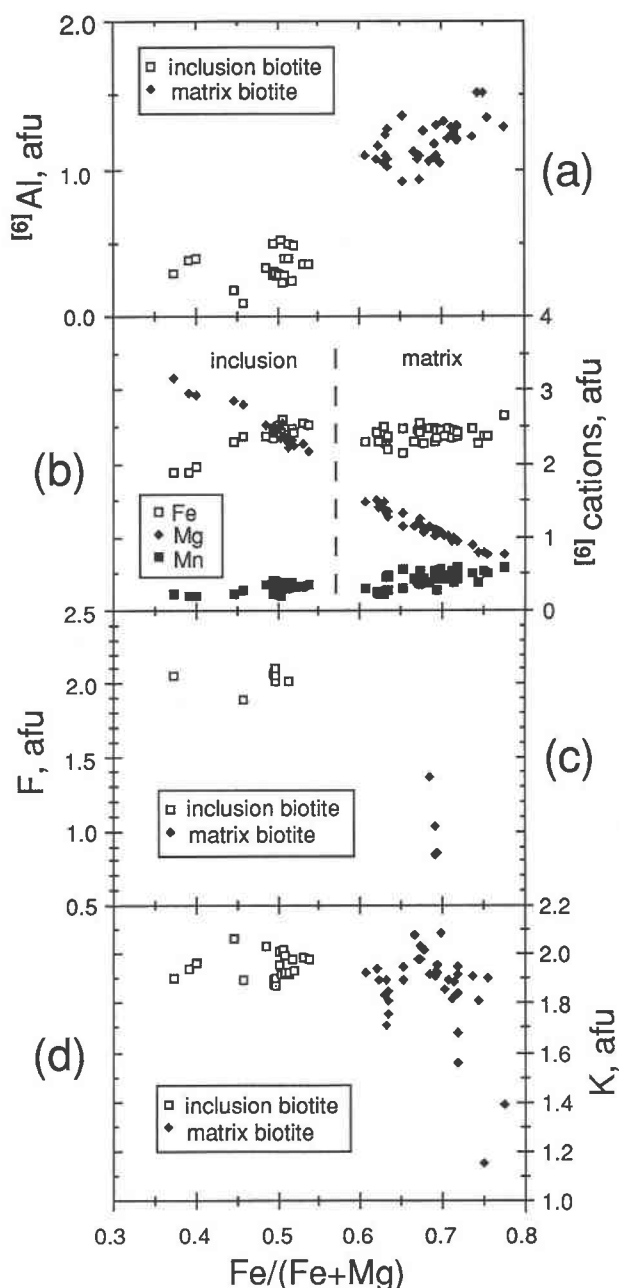
Fig. 4. Variation diagrams of (a) [6]Al, (b) Fe, Mg, Mn, (c) F, and (d) K with Fe/(Fe + Mg) for the Cuffytown Creek pluton biotite; afu = atomic formula units.

by a zinnwaldite substitution. If all the 20–40 ppm of Li reported for the rocks (Speer and Becker, 1990) is present in the biotite, it would correspond to 0.4–0.8 wt% Li_2O. If some Li_2O is partitioned into the white micas, Li_2O in biotite would be small, less than 0.2 wt%.

Muscovite

White mica is the most abundant varietal mineral in the Cuffytown Creek granites, constituting up to 3.7 modal% of the rock. It is pleochroic (colorless to very pale
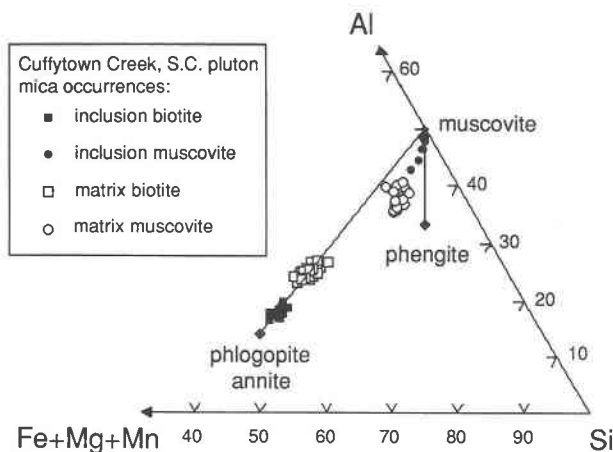
Fig. 5. Cuffytown Creek pluton mica compositions plotted as atomic proportions of (Fe + Mg + Mn)-Al-Si. Biotite shows primarily dioctahedral substitution, muscovite a combination of trioctahedral and celadonite substitutions.

yellowish brown) in thin section. White mica occurs as anhedral grains up to 3 mm that are interstitial to quartz and feldspar (Fig. 2d). Inclusions of white mica occur in quartz (Fig. 2c), but they are less common than inclusion biotite. The other, and most common, occurrence of white mica is as replacements of other minerals. White mica grains interleaved with biotite + chlorite (Fig. 2a) or chlorite (Fig. 2e) and hematite + rutile ± fluorite are interpreted as replacements or pseudomorphs of biotite. White mica replaces plagioclase, either as single large grains (Fig. 2f) or as fine-grained random or oriented flakes (Fig. 2g). Garnet is also replaced by white mica (Fig. 2h).

Microprobe analyses show that the Cuffytown Creek white micas are muscovite and phengite (Appendix 1, Table 2). The white micas plot between the muscovite-phengite and dioctahedral-trioctahedral joins on a M-Al-Si (atomic proportion) diagram (Fig. 5). This indicates that celadonite, $(Fe^{2+},Mg,Mn)Si^{[6]}Al_{-1}{}^{[4]}Al_{-1}$, and diocta-hedral-trioctahedral substitutions, $(Fe^{2+},Mg,Mn)_3{}^{[6]}Al_{-2}$-$^{[6]}\square_{-1}$, are equally important. Matrix white mica is phengite, with 6.15–6.64 Si afu (ave. 6.46), whereas inclusion white mica is slightly, but distinctly, more muscovite rich, with 6.08–6.25 Si afu (ave. 6.17), and has greater octahedral Al occupancy (Figs. 5, 6a). Inclusion white mica has Fe/(Fe + Mg) = 0.90–0.99, ave. 0.95, whereas the matrix white mica is more magnesian, with Fe/(Fe + Mg) = 0.61–0.78, ave. 0.67. However, Fe content of the matrix white mica is greater than the inclusion white mica; Fe/(Fe + Mg) is less only because the inclusion white mica has little Mg and Mn (Fig. 6b). Inclusion white mica also differs from matrix muscovite in containing less F, but more K and Na (Figs. 6c, 6d). Inclusion white mica has less Ti (ave. 0.015 afu) than the matrix white mica (ave. 0.058 afu). As is the case for the biotite, the Li_2O content is interpreted to be low.
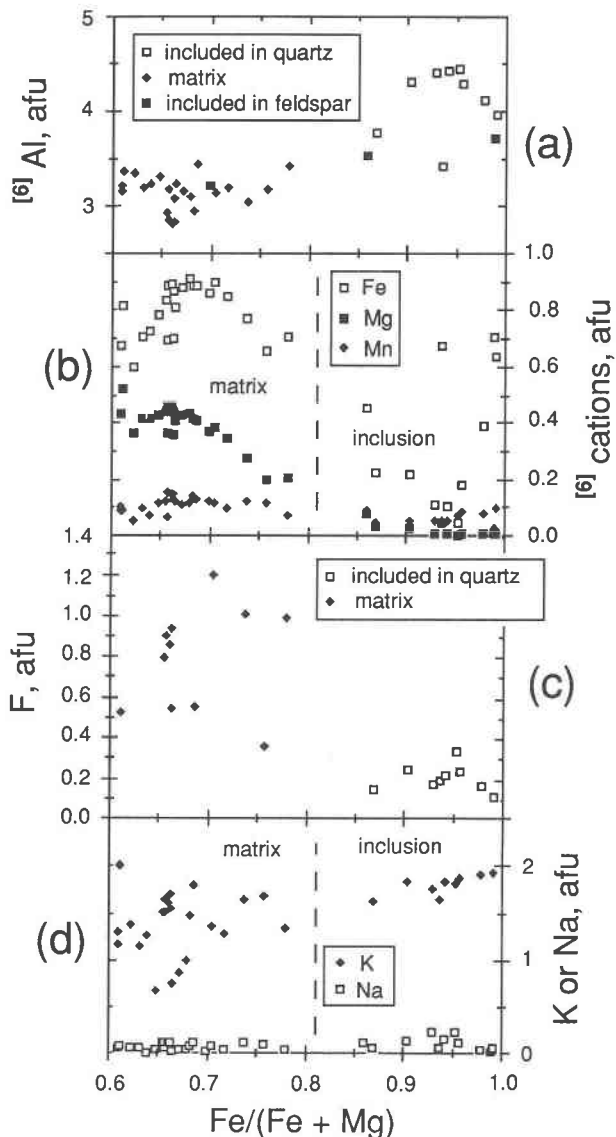
Fig. 6. Variation diagrams of (a) $^{[6]}Al$, (b) Fe, Mg, and Mn, (c) F, and (d) Na and K with Fe/(Fe + Mg) for the Cuffytown Creek pluton muscovite; afu = atomic formula units.

Garnet

Garnet crystals are light brown and less than 1 mm across. They are interstitial and anhedral, with locally abundant oxide mineral inclusions, forming late during the crystallization of the leucocratic minerals. Only in late dike rocks did garnet grow contemporaneously with much of the feldspar and quartz and form euhedral crystals. The textural relationship with fluorite is less certain: garnet forms both overgrowths on euhedral fluorite and intergrowths with fluorite. Garnet is replaced by white mica (Fig. 2h) and white mica + carbonate minerals.

Cuffytown Creek garnet is spessartine-almandine, containing between 67 and 78 mol% spessartine (Appendix

1, Table 3). Ca and Mg are minor, with less than 5.6 mol% grossular + andradite and less than 3.0 mol% pyrope. The average composition is $Alm_{23.4}Py_{2.0}Sp_{73.1}Gr + Adr_{1.5}$. Slight zoning is present in some grains: rims are more calcic (≈ 1 mol%) but can be either more Fe rich (≈ 5 mol% almandine, CB7-15) or more Mn rich (≈ 2 mol% spessartine, S7-50a, ED1-872) than cores. The garnet contains up to 1.0 wt% F.

Other minerals

Fluorite is present in all samples and constitutes up to 1 modal% of the rock, an amount subequal to the varietal minerals. The most abundant fluorite is found as anhedral grains interstitial to the feldspars and quartz and contains abundant opaque inclusions, which are locally altered to chlorite + muscovite. Fluorite also replaces biotite and plagioclase (Fig. 2f) and occurs as euhedral crystals growing into interstitial white mica or carbonate minerals.

Chlorite occurs interlayered with biotite and muscovite (Fig. 2a), with muscovite as pseudomorphs of biotite (Fig. 2e), and as a replacement of plagioclase (Fig. 2g) and opaques. Microprobe analyses (Appendix 1, Table 4) show the chlorite has Fe/(Fe + Mg) between 0.79 and 0.99 and between 5.3 and 5.6 Si afu. Chlorite with Fe/(Fe + Mg) > 0.98 replaces and pseudomorphs magnetite.

Ferroan rhodochrosite (64.9% rhodochrosite, 23.3% siderite, 11.7% calcite, and 0.1% magnesite, Appendix 1) is interstitial to the other minerals and anhedral against white mica, fluorite, and albite. It widely replaces plagioclase and garnet.

The major igneous oxide opaque assemblage is magnetite + ilmenite and occurs as inclusions in all other minerals. Ilmenite is partially to entirely altered to rutile + hematite; magnetite grains have been replaced to varying degrees by hematite and chlorite + muscovite. Analyses of the oxides (Appendix 1) show that the hematite and magnetite are nearly end-member compositions but ilmenites contain up to 4 wt% MnO.

DISCUSSION

AFMMn crystallization sequence

Inclusions of biotite and muscovite in quartz are interpreted as an early AFMMn liquidus assemblage (A = Al_2O_3-K_2O-Na_2O-CaO, F = FeO, M = MgO, Mn = MnO, in molecular amounts). The much greater abundance of biotite inclusions relative to muscovite may mean that biotite started to crystallize before muscovite. The matrix assemblage biotite + muscovite ± garnet is a later AFMMn liquidus assemblage. Replacement of biotite by coarse-grained muscovite is interpreted as a reaction leading to the disappearance of biotite and the last liquidus AFMMn assemblage: muscovite + garnet. These minerals persisted into the subsolidus, where they changed composition, recrystallized, or were replaced. Other minerals that appeared in the subsolidus are chlorite, ferroan
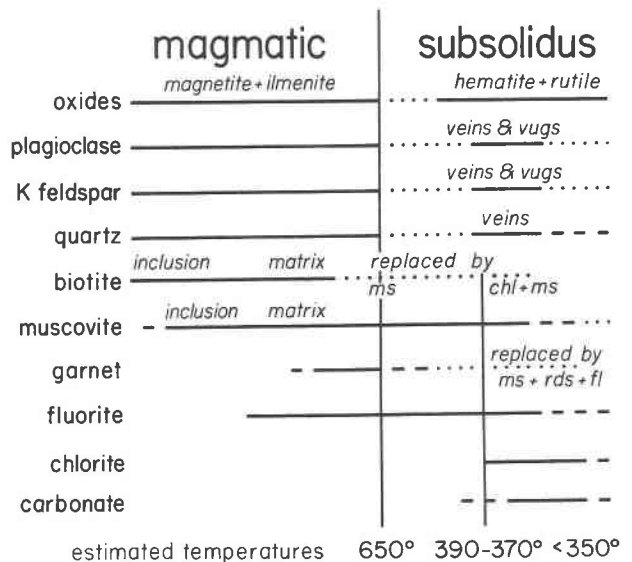
Fig. 7. Sequence of magmatic and subsolidus crystallization for the Cuffytown Creek pluton, South Carolina. The event defining the end of the magmatic stage, and represented by the longer vertical line in the center, is complete crystallization of the nonvein quartz and feldspar. The shorter vertical line under subsolidus is the replacement of biotite by muscovite + chlorite, Reaction 4.

rhodochrosite, rutile, and hematite. The sequence of liquidus and subsolidus mineral formation in the Cuffytown Creek pluton, based on the textural and compositional information, is summarized in Figure 7. Two assumptions were used in constructing the diagram: (1) nonvein quartz and feldspars finished crystallization at the same time, an event that defined the end of magmatic processes; and (2) replacement of biotite by muscovite + chlorite is a subsolidus reaction that resulted in the disappearance of biotite and the appearance of chlorite.

Figure 8a is a graphical summary of the liquidus AFMMn mineral compositions. It includes the early-formed inclusion micas, but tie lines are drawn for the three-phase AFMMn matrix assemblage biotite + muscovite + garnet. The matrix assemblage is the major one preserved in the granites, although their compositions may reflect subsolidus reequilibration. Compositions of the three-phase subsolidus AFMMn reaction assemblage leading to the disappearance of biotite, biotite + chlorite + muscovite, are presented in Figure 8b. This is a widespread assemblage and, because the minerals are intergrown, the only subsolidus assemblage whose compositions are reliably known to coexist.

AFMMn crystallization reactions

Liquidus reactions for muscovite- and garnet-bearing granites are described by Miller and Stoddard (1980, 1981), Abbott (1981a, 1981b, 1985), and Zen (1988). They propose that an original biotite-bearing granite melt would
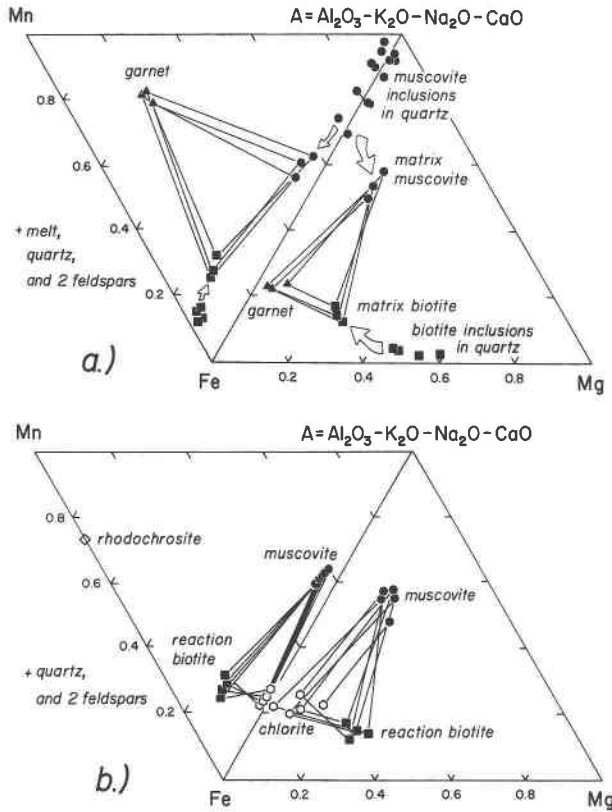
Fig. 8. Summary AFMMn (A = mol Al₂O₃-K₂O-Na₂O-CaO, F = mol FeO, M = mol MgO, Mn = mol MnO) diagram projected from quartz, alkali feldspar, plagioclase, and H₂O. (a) The two liquidus AFMMn assemblages: early inclusion biotite and muscovite and the matrix biotite + muscovite + garnet formed toward the end of magmatic crystallization. (b) The subsolidus AFMMn assemblage biotite + chlorite + muscovite; this is the reaction assemblage leading to the disappearance of biotite.

Fig. 9. (a) Possible A-Fe-Mg-Mn liquidus topology based on Abbott (1981b, 1985). (b) Same diagram with the compositions of the Cuffytown Creek minerals and possible melt evolution.

evolve in the sequence liquid = Bt to liquid = Bt + Ms to liquid + Bt = Ms + Grt or liquid + Bt + Ms = Grt and finish with liquid + Ms = Grt or liquid = Ms + Grt. The crystallization sequence of liquidus AFMMn assemblages in the Cuffytown Creek is biotite (?), biotite + muscovite, biotite + muscovite + garnet, and muscovite + garnet. This specific sequence of assemblages is broadly predicted by all authors, but the crystallization reactions may differ. The Cuffytown Creek pluton crystallization is examined in terms of Abbott's (1981b, 1985) topologies (Fig. 9a) because more and specific predictions are made for these. An additional attraction is that his topologies can be expanded to other crystallization conditions or granite compositions (cf. Speer, 1987).

Figure 9b is a plot of the Cuffytown Creek rock and mineral compositions on Abbott's (1981b, 1985) AFMMn liquidus topology. Also included is a possible liquid line of descent for the melt, $l_1l_2l_3l_4l_5$, consisting of four segments. The first segment is crystallization of the inclusion biotite by the reaction liquid = Bt. The beginning melt composition, l_1, must be located at Fe/(Fe + Mg) values

greater than that of the inclusion biotite (= 0.37–0.54) because magnetite, a ferrous phase not normally included in AFMMn diagrams, is also crystallizing. Crystallization of the relatively Mg-rich, alumina-poor biotite moves the melt composition toward the three-phase liquid-Bt-Ms surface along the path l_1-l_2.

Once encountering the three-phase liquid-Bt-Ms surface at l_2, the melt crystallizes muscovite as well as biotite. Because muscovite inclusions in quartz are much less common than biotite inclusions, the liquid = Bt + Ms crystallization reaction must have begun toward the end of quartz crystallization or only in scattered locations in the magma. Crystallization of the two micas, which together have high magnesia and alumina contents and low Mn/(Fe + Mg + Mn), must enrich the melt in Mn/(Fe + Mg + Mn) and Fe/(Fe + Mg + Mn) while decreasing A (A = Al₂O₃-K₂O-Na₂O-CaO). The melt moves along the three-phase surface liquid-Bt-Ms, away from the bi-

otite-muscovite (± magnetite) join and toward the four-phase equilibrium liquid-Bt-Grt-Ms along the path, l_2-l_3.

Where the liquid composition encounters the four-phase equilibrium liquid-Bt-Grt-Ms determines the reaction responsible for the matrix AFMMn liquidus assemblage biotite + muscovite + garnet. Along x-x' the crystallization reaction is liquid + Bt + Ms = Grt, whereas along x'-x'' the reaction is liquid + Bt = Ms + Grt. Replacement of biotite by muscovite indicates the latter reaction and that l_3 must lie on the segment x'-x''. Appearance of garnet represents the first crystallization of an Mn-rich phase, but modal abundances are muscovite > biotite ≫ garnet. Thus continued crystallization of greater amounts of Mn-poor biotite, muscovite, and oxides still would allow the melt to become richer in Mn/(Fe + Mn) between l_3 and l_4.

Once biotite is consumed, the melt leaves the four-phase equilibrium liquid-Bt-Ms-Grt at l_4 and moves along the three-phase surface liquid-Ms-Grt. The reaction on this surface is either liquid + Ms = Grt, at low-Mn/(Fe + Mn) and high temperatures, or liquid = Grt + Ms, at high Mn/(Fe + Mn) and low temperatures (Fig. 9a). The two possibilities result from the surface intersecting the almandine-spessartine join (Abbott, 1981b). In the Cuffytown Creek pluton, there is no textural evidence from the muscovite and garnet to determine the reaction relations. However, the compositions of the Cuffytown Creek garnets are confined to below the equilibrium liquid-Grt-Ms surface (Fig. 9b), and the immediately previous crystallization reaction is liquid + Bt = Ms + Grt along the segment x'-x''. Both of these indicate that the final crystallization reaction was liquid = Grt + Ms along the path segment l_4l_5. The last melt composition is l_5, on the compositional join of the last garnet + muscovite.

Compositional variations in micas and garnet

The inclusion biotite samples show both $FeMg_{-1}$ and $Mn(Fe,Mg)_{-1}$ exchanges (Fig. 4b). We are unable to tell on textural grounds which among the inclusion biotite samples are the earlier biotite; however, the melt probably becomes increasingly Mn rich with crystallization so that the magnesian, Mn-poor biotite is probably the first to crystallize. With no other compositional variations evident for the inclusion biotite, the crystallization reaction was liquid = Bt[$FeMg_{-1}$,$Mn(FeMg)_{-1}$] ± Ms. Instead of interpreting the biotite $FeMg_{-1}$ as reflecting change in melt $FeMg_{-1}$, it could be interpreted as cooling of the reaction assemblage biotite + alkali feldspar + magnetite + fluid along an f_{O_2} buffer (Wones and Eugster, 1965). However, the two interpretations may be one and the same for a closed-system melt cooling along an O buffer. The Cuffytown Creek pluton, with its coexisting Fe-Ti oxides, appears to meet this criterion.

The later matrix biotite differs from inclusion biotite in that it is higher in [6]Al and Mn and lower in Mg and F (Fig. 4). As discussed below, the matrix-mineral compositions may be in part subsolidus. However, their compositions lie on the original igneous trends, and we inter-

pret the broad compositional differences between the inclusion and matrix minerals as indicating in a general way compositional differences between the inclusion- and matrix-liquidus assemblages. If so, a more complete expression of the transition from the inclusion- to matrix-biotite crystallization reaction is
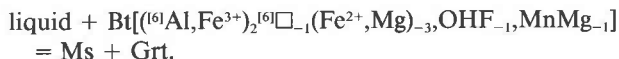
liquid + Bt[($^{[6]}$Al,Fe^{3+})$_2$$^{[6]}$□$_{-1}(Fe^{2+},Mg)_{-3}$,OHF$_{-1}$,MnMg$_{-1}$] = Ms + Grt.

White inclusion micas have little compositional variation, so it would appear that early magmatic white micas were uniformly ideal muscovite in composition. With evolution to the matrix assemblages, the white micas show celadonite, di-trioctahedral, K, and F substitutions, indicating the crystallization reaction

liquid + Bt = Ms[(Fe^{2+},Mg,Mn)Si$^{[6]}$Al$_{-1}$$^{[4]}Al_{-1}$,(Fe^{2+},Mg,Mn)$_3$-$^{[6]}Al_{-2}$$^{[6]}$□$_{-1}$,OHF$_{-1}$,KNa$_{-1}$] + Grt.
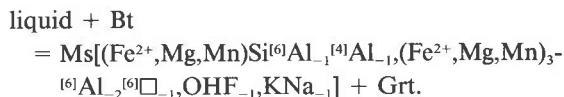
White micas increase their Fe and Mg contents with crystallization, but Fe/(Fe + Mg) decreases (Fig. 6b). More importantly, the Cuffytown Creek white micas evolve from muscovite to phengite (Fig. 5). This is anticipated from the experimental work of Monier and Robert (1986b), who found that high-temperature (magmatic) white micas are muscovite whereas low-temperature (subsolidus) white micas are more phengitic with a trioctahedral component, and become increasingly so with decreasing temperatures. The lesser Na content of the matrix phengite is difficult to interpret. Although muscovite coexisting with paragonite would be expected to decrease its Na content with decreasing temperature because of the widening of the muscovite + paragonite solvus, Na should increase with decreasing temperature in muscovite coexisting with feldspar (Evans and Guidotti, 1965) or as the feldspar and melt become more sodic with fractional crystallization (Thompson and Tracy, 1979).

Ti contents of white mica have been used, along with other criteria, to distinguish magmatic from subsolidus white micas (Speer, 1984). No limits are established, but the range of Ti contents in the Cuffytown Creek matrix phengite (0.058–0.083 afu) is comparable to that in white micas interpreted as magmatic elsewhere (Miller et al., 1981; Monier and Robert, 1986a). The inclusion muscovite has a much lower range of Ti contents (0.001–0.047 afu) that overlap the compositions of other subsolidus white micas, but the textural and phase stability evidence in this case is that they are magmatic. The use of Ti content as a criterion for magmatic muscovite may depend on specifying melt composition, phase assemblage, or physical conditions.

We interpret the garnet as magmatic because of its inclusion in magmatic minerals. The widespread, uniform occurrence of garnet is an additional reason for interpreting the garnet as magmatic: it is not restricted in occurrence to contact zones, fractures, or late pegmatites, as is garnet interpreted as postmagmatic in other granites (Kontak and Corey, 1988; Puziewicz, 1990). Abbott's

(1981b, 1985) topologies predict an early Fe-rich garnet that evolves to a more Mn-rich composition with crystallization. The uniform and virtually unzoned garnet compositions in the Cuffytown Creek granites indicate that either garnet crystallized at the same time or early-formed Fe-rich garnet subsequently reequilibrated with later and more Mn-rich melts. Yardley (1977) and Woodsworth (1977) have shown that garnet zoning in metamorphic rocks can be eradicated in garnets at temperatures between 550 and 700 °C, most likely starting at 600 °C. Thus reequilibration of an original Fe-rich garnet with Mn-rich melt could occur during the magmatic history of the Cuffytown Creek, if cooling rates were sufficiently slow. If there is continued reequilibration, the melt does not have to be extremely Mn rich when garnet first appears.

Subsolidus reactions

Subsolidus reactions of the felsic minerals center on exsolution of the alkali feldspar and replacement of plagioclase by muscovite and fluorite. Muscovite and fluorite could be simple replacement products, with sodic plagioclase serving only as a nucleation site. In this case, all material required to form muscovite and fluorite or in excess must be supplied and removed by the fluid. The other extreme is that the more calcic plagioclase in the Cuffytown Creek granite was a reactant and that the fluid supplied and removed only minimal material (in wt%):

feldspar components (3.23 Ab + 43.26 An
+ 43.06 Or) + fluid (0.10 H_2O + 6.38 F)
+ 0.62 MnO + 3.04 FeO + 0.31 MgO
+ 0.04 TiO_2
    = 74.34 muscovite (S7-55) + 13.78 quartz
        + 11.88 fluorite.   (1)
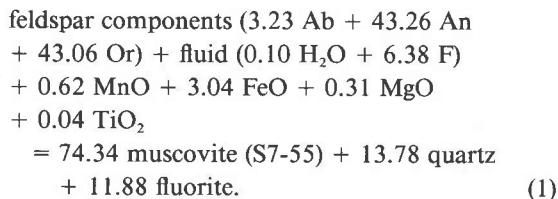
The material necessary to form the relatively small amounts of muscovite and fluorite can be supplied by the feldspar and oxide minerals with the fluid supplying volatiles. A similar reaction was proposed by Exley (1958), who found that if the Ca contained in fluorite were returned to the plagioclase, its competition would be the same as that of the plagioclase in related granites without fluorite.

The most noticeable subsolidus reaction texture of the AFMMn minerals is replacement of biotite by chlorite + phengite. Assuming that hydration accompanies a decrease in temperature, compositional relations of the three-phase subsolidus assemblage biotite + chlorite + phengite indicate a continuous reaction of the general type Bt = Chl + Ms (Fig. 8b). To write a balanced reaction, large amounts of silica and alumina are needed. These could be brought in by the fluid, but what is more probable is that the fluid supplied only the volatiles and the other components were derived from the minerals present in the rock. Feldspars are the most logical source of both alumina and silica, and the reaction would be

feldspar components (2.67 Ab + 32.26 An
+ 19.13 Or) + 40.99 matrix biotite (S7-55)
+ fluid (4.95 F)
    = 83.15 matrix phengite (S7-55)
        + 3.58 chlorite (S7-55) + 4.39 quartz
        + 8.88 fluorite.   (2)
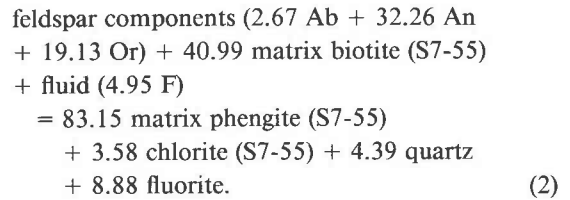
Reaction 2 is written to be discontinuous. Because muscovite is concluded to be a magmatic phase, it also must be involved as a reactant. In addition, matrix biotite and chlorite change compositions continuously; hence they are involved both as reactants and products in a continuous reaction. Based on the compositions of biotite + chlorite + phengite, the reactants and products of Reaction 2 should move toward more magnesian compositions. This compositional shift is most obvious in the higher magnesian contents of matrix or subsolidus phengite as compared to the inclusion muscovite (Fig. 6b). It is more difficult to show in the chlorites and biotite because of uncertain age relations and the oxidation of Fe in the biotite. However, a chlorite + muscovite assemblage is much more magnesian than the chlorite + muscovite + biotite assemblages (Fig. 8b). Because we do not know the original compositions of the biotite, chlorite, and muscovite, a continuous reaction cannot be written and balanced using observed mineral compositions (Hensen, 1980). However, the continuous reaction version of Reaction 2 can be qualitatively written as

feldspars + iron biotite + muscovite
+ iron chlorite + fluid
    = albite + magnesium biotite + phengite
        + magnesium chlorite + fluorite + quartz.   (3)
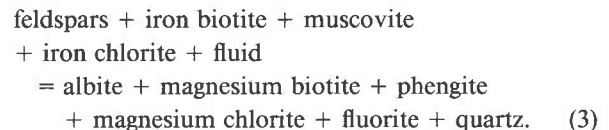
This reaction is a combination of both net transfer Reactions 1 and 2 as well as the exchange reaction $(Fe^{2+},Mn)Mg_{-1}$. It describes the replacement of the igneous, quartz-bearing assemblage plagioclase + alkali feldspar + biotite + muscovite + fluid by the subsolidus, quartz-bearing assemblage albite + potassium feldspar + chlorite + muscovite + fluorite.

Textural evidence indicates that garnet persisted from magmatic conditions through conditions of Reaction 3 in the subsolidus. Subsequent to the replacement of biotite by chlorite + muscovite, garnet is replaced by muscovite + rhodochrosite:

50.84 garnet (S7-55) + 30.27 alkali feldspar
+ fluid (1.22 F + 0.28 H_2O + 15.42 CO_2)
    = 49.25 muscovite (S7-55)
        + 35.88 rhodochrosite (ED1-872)
        + 14.86 quartz.   (4)
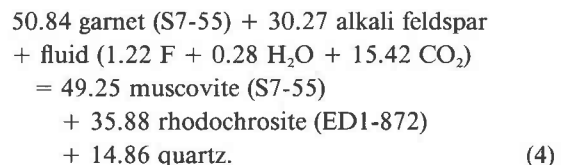
Reaction 4 is written as a discontinuous reaction but is most likely a continuous one.

Other relatively high-temperature subsolidus reactions include exsolution of ilmenite and its subsequent oxidation to hematite + rutile. Although the timing of this

replacement is not well known, the widespread occurrence of ilmenite pseudomorphs as inclusions in both magmatic and subsolidus minerals indicates it is late. Low-temperature subsolidus reactions include replacement of alkali feldspar by hematite-bearing dusty inclusions and formation of iron and manganese oxides and hydroxides that line grain boundaries and cleavage traces. The abundant dendrites of manganese hydroxides + pyrophyllite observed in fractures (Speer and Becker, 1990) appear to derive their Mn and Fe from the easily soluble rhodochrosite.

Melt phase

The compositionally least-constrained phase of the crystallization reactions is the melt. However, compositional limits can be placed on the melt using the mineral compositions and the topology of Figure 9. The Fe/(Fe + Mg) composition of the original melt would lie between the two early Fe phases: magnetite (1.0) and inclusion biotite (0.37), but after the early and abundant crystallization of magnetite it was probably closer to that of the biotite. With crystallization of the assemblage liquid + Bt + Ms + Grt, Fe/(Fe + Mg) increased to between 0.7 and 0.85. After biotite disappeared, it may have increased to values as high as 0.95, which is the average composition of the last two crystallizing AFMMn phases, garnet and inclusion muscovite. The Mn/(Fe + Mn) of the early Cuffytown Creek melt was between that of the inclusion biotite (0.1) and the first appearance of the assemblage liquid + Bt + Ms + Grt (0.2). Once biotite disappeared, Mn/(Fe + Mn) increased to values greater than the tie line between the garnets (0.78) and muscovite ($\leq$0.33). The Al content of the melt is only broadly constrained. During crystallization of the inclusion biotite, A/(FMMn) $\geq$ 0.015. During crystallization of the final muscovite + garnet assemblage, A/(FMMn) increased to a value between garnet (0.28) and muscovite (0.55). Based on Abbott's (1981a) topologies, the value was closer to 0.28.

Volatile components

Compositions of the micas and the abundance of fluorite show that both H_2O and F were important volatile components of the melt. The abundance of F is also shown by garnet containing up to 0.9 wt% F. By all indications, Cl was present in only small amounts throughout. If the vugs are correctly interpreted as miarolitic cavities, P_{fluid} = P_{tot} at the end of magmatic crystallization and the beginning of the subsolidus and the volatiles constituted a separate phase. Based on the experimental work of Webster (1990), the fluid must have also contained components of the silicate melt. This fluid would have persisted into the subsolidus when it evolved into or mixed with any postmagmatic hydrothermal, pneumatolytic, or deuteric fluids (Webster, 1990). In the subsolidus, carbonate minerals crystallize, and carbon dioxide was an additional important constituent of the volatile phase.

Physical conditions

The magmatic stage in the Cuffytown Creek pluton could persist to temperatures as low as 650 °C on the basis of experiments with high F granitic melts, both wet (Manning, 1981) and dry (Snow and Kidman, 1990). Pluton emplacement pressure was estimated by Speer and Becker (1990) at 1–4 kbar on the basis of normative Q + Ab + Or compositions. If competing compositional effects of Ca, F, and $P_{H_2O} < P_{tot}$ balance one another, the estimate can be narrowed to 2–3 kbar.

Subsolidus temperatures can be estimated from mineral pair geothermometers. Feldspar geothermometry yields temperatures in the range of 345–392 °C, using the parameters of Elkins and Grove (1990) and the algorithms of Fuhrman and Lindsley (1988). Feldspar pairs more sodic than Or_{93} and An_5 have discordant temperatures. The plagioclase-muscovite thermometer (Green and Usdansky, 1986) gives temperatures in the range of 319–483 °C. Chlorite thermometry yields average temperature estimates of 262 °C (Cathelineau and Nieva, 1985) and 336 °C (Cathelineau, 1988); in both cases the range is less than ±10 °C. Desborough et al. (1980) relied on a reaction similar to Reaction 2 to explain reequilibration of feldspars to subsolidus temperatures in the Redskin alkali feldspar granite. In the case of the Cuffytown Creek pluton, the two-feldspar, plagioclase-muscovite, and chlorite equilibria pertain to Reaction 3.

Broad constraints on subsolidus temperatures can also be derived from experimental phase equilibria. The Fe-free equilibrium Bt + Kfs + Qz + H_2O = Ms, which is a component reaction of Reaction 2, has three brackets: 375–390 °C at 2 kbar (Velde, 1965), 350–450 at 4 kbar (Massone, 1981), 440–480 °C at 4.5 kbar (Velde, 1965). The low-temperature stability of spessartine is the reaction Sps + fluid = Mn-chl + Qz + fluid at 400 °C at 2 kbar; addition of Fe increases the temperature of reaction to 550–600 °C, depending on the f_{O_2} (Hsu, 1968). Experimental study of muscovite with celadonite and dioctahedral substitutions comparable to those found in the Cuffytown Creek pluton show that they have thermal stabilities at 300–400 °C (Monier and Robert, 1986a).

Oxygen fugacity estimates cannot be made because the nearly end-member compositions of the magnetite and ilmenite indicate equilibration outside the calibration of the Fe-Ti oxide thermobarometer. Qualitatively, the magnetite + ilmenite assemblage indicates a magmatic f_{O_2} between conditions of the hematite + magnetite and quartz + fayalite + magnetite buffers. Formation of a hematite + rutile subsolidus assemblage indicates that f_{O_2} increased in the subsolidus.

Values of $\log(f_{H_2O}/f_{HF})$ calculated from the inclusion micas, using the formulas of Gunow et al. (1980) and assuming a temperature of 650 °C, are 3.04–3.25 for the inclusion biotite samples, and 3.27–3.87 for inclusion muscovite samples. Within uncertainties of the mineral analyses and calculations these values are probably identical. Values of $\log(f_{H_2O}/f_{HF})$ calculated for the matrix mi-

cas, assuming an exchange temperature of 350 °C, are 4.21–4.48 for the biotite samples and 3.91–5.02 for the white micas. Calculation of relative $\log(f_{HF}/f_{HCl})$ values (Munoz and Swenson, 1981), based on an equilibration temperature of 350 °C, yields estimates of between 0.5 and −0.5. These fugacity ratios pertain to Reaction 2, the buffering reaction for the fluid in the subsolidus. However, the large range for white micas may result from their involvement in other subsolidus reactions such as 1 and 4 or perhaps from relict igneous compositions. The (f_{H_2O}/f_{HF}) values indicate an increase in f_{H_2O} relative to f_{HF} from the magmatic to subsolidus stages.

The appearance of rhodochrosite late in the subsolidus suggests low amounts of CO_2 in the fluid until that time. The stability of $MnCO_3$ + quartz at temperatures less than 400 °C indicates $X_{CO_2} > 0.1$ in an aqueous fluid (Candia et al., 1975; Abrecht, 1988). The preservation of rhodochrosite without decomposition to an oxide at temperatures <400 °C until weathering indicates $\log f_{O_2} < -8$ atm (Huebner, 1969).

CONCLUSIONS

1. The sequence of liquidus AFMMn assemblages in the Cuffytown Creek alkali feldspar granites is biotite (?), biotite + muscovite, biotite + muscovite + garnet, and muscovite + garnet corresponding to the reactions liquid = Bt, liquid = Bt + Ms, liquid + Bt = Ms + Grt, and, finally, liquid = Grt + Ms. Bt ± Ms are preserved as inclusion assemblages in quartz, whereas Bt + Ms + Grt and Grt + Ms are the matrix AFMMn assemblages.

2. Inclusion biotite $FeMg_{-1}$ and $Mn(Fe,Mg)_{-1}$ variations reflect change in melt $FeMg_{-1}$ caused by a likely combination of crystallization of magnesian minerals and cooling along an f_{O_2} buffer. From the early magmatic through late magmatic to subsolidus stages, the compositional gap between the di- and trioctahedral micas narrows. White mica Ti content increases from what would be considered nonmagmatic values in the inclusion muscovite to magmatic values in the matrix phengite and may depend on melt composition or phase assemblage in addition to temperature. Garnets have relatively uniform and homogeneous compositions, indicating the garnets either crystallized largely at one set of conditions or at temperatures where garnet zoning is erased by diffusion.

3. The predicted liquid line of descent indicates the melt becomes increasingly rich in Fe/(Fe + Mg + Mn) and Mn/(Fe + Mg + Mn) with decreasing temperatures, but each does so at differing rates at different stages during crystallization. Melt peraluminosity increases rapidly with crystallization of biotite, then decreases slightly during crystallization of Bt + Ms, before increasing at a much slower rate with crystallization of Bt + Ms + Grt and Ms + Grt.

4. The subsolidus assemblage phengite + chlorite + potassium feldspar + albite + rhodochrosite + fluorite + quartz results from two reactions that occur at ≈300–400 °C: (1) plagioclase + iron biotite + muscovite + iron chlorite + fluid = albite + potassium feldspar + magnesium biotite + phengite + magnesium chlorite + fluorite + quartz, and (2) garnet + potassium feldspar + fluid = muscovite + rhodochrosite + quartz.

REFERENCES CITED

Abbott, R.N., Jr. (1981a) AFM liquidus projections for granitic magmas, with special reference to hornblende, biotite and garnet. Canadian Mineralogist, 19, 103–110.
——— (1981b) The role of manganese in the paragenesis of magmatic garnet: An example from the Old Woman–Puite Range, California: A discussion. Journal of Geology, 89, 767–769.
——— (1985) Muscovite-bearing granites in the AFM liquidus projection. Canadian Mineralogist, 23, 553–561.
Abrecht, J. (1988) Experimental evaluation of the $MnCO_3$ + SiO_2 = $MnSiO_3$ + CO_2 equilibrium at 1 kbar. American Mineralogist, 73, 1285–1291.
Candia, M.A.F., Peters, Tj., and Valarelli, J.V. (1975) The experimental investigations of the reactions $MnCO_3$ + SiO_2 = $MnSiO_3$ + CO_2 and $MnCO_3$ + $MnSiO_3$ = Mn_2SiO_4 + CO_2 in CO_2/H_2O gas mixtures at a total pressure of 550 bars. Contributions to Mineralogy and Petrology, 52, 261–266.
Cathelineau, M. (1988) Cation site occupancy in chlorites and illites as a function of temperature. Clay Minerals, 23, 471–485.
Cathelineau, M., and Nieva, D. (1985) A chlorite solid solution geothermometer, the Los Azufres (Mexico) geothermal system. Contributions to Mineralogy and Petrology, 91, 235–244.
Desborough, G.A., Ludington, S.D., and Sharp, W.N. (1980) Redskin Granite: A rare-metal Precambrian pluton, Colorado, USA. Mineralogical Magazine, 43, 959–966.
Elkins, L.T., and Grove, T.L. (1990) Ternary feldspar experiments and thermodynamic models. American Mineralogist, 75, 544–559.
Evans, B.W., and Guidotti, C.V. (1965) The sillimanite-potash feldspar isograd in western Maine, U.S.A. Contributions to Mineralogy and Petrology, 12, 25–62.
Exley, C.S. (1958) Magmatic differentiation and alteration in the St. Austell granite. Quarterly Journal of the Geological Society of London, 114, 197–230.
Fuhrman, M.L., and Lindsley, D.H. (1988) Ternary-feldspar modeling and thermometry. American Mineralogist, 73, 201–215.
Green, N.L., and Usdansky, S.I. (1986) Toward a practical plagioclase-muscovite thermometer. American Mineralogist, 71, 1109–1117.
Gunow, A.J., Ludington, A., and Munoz, J.L. (1980) Fluorine in micas from the Henderson molybdenite deposit, Colorado. Economic Geology, 75, 1127–1137.
Hensen, B.L. (1980) The use of petrological mixing models for the evaluation of reactions in metamorphic rocks—A comment on a paper by R.W. LeMaitre. Contributions to Mineralogy and Petrology, 74, 103–104.
Hsu, L.C. (1968) Selected phase relationships in the system Al-Mg-Fe-Si-O-H: A model for garnet equilibria. Journal of Petrology, 9, 40–83.
Huebner, J.S. (1969) Stability relations of rhodochrosite in the system manganese-carbon-oxygen. American Mineralogist, 54, 457–481.
Kontak, D.J., and Corey, M. (1988) Metasomatic origin of spessartine-rich garnet in the South Mountain Batholith, Nova Scotia. Canadian Mineralogist, 26, 315–334.

Kretz, R. (1983) Symbols for rock-forming minerals. American Mineralogist, 68, 277–279.

Manning, D.A.C. (1981) The effect of fluorine on liquidus phase relationships in the system Qz-Ab-An with excess water at 1 kb. Contributions to Mineralogy and Petrology, 76, 206–215.

Massone, H.J. (1981) Phengite: Eine experimentelle Untersuchung ihres Druck-Temperatur-Verhaltens im System K_2O-MgO-Al_2O_3-SiO_2-H_2O. Unpublished Ph.D. thesis, University of Bochum, Bochum, Germany (not seen, extracted from Contributions to Mineralogy and Petrology, 96, 519–522, 1987).

Miller, C.F., and Stoddard, E.F. (1980) The role of manganese in the paragenesis of magmatic garnet: An example from the Old Woman–Puite Range, California. Journal of Geology, 89, 233–246.

——— (1981) The role of manganese in the paragenesis of magmatic garnet: An example from the Old Woman–Puite Range, California: A reply. Journal of Geology, 89, 770–772.

Miller, C.F., Stoddard, E.F., Bradfish, L.J., and Dollase, W.A. (1981) Composition of plutonic muscovite: Genetic implications. Canadian Mineralogist, 19, 25–34.

Monier, G., and Robert, J.-L. (1986a) Titanium in muscovites from two mica granites: Substitutional mechanism and partition with coexisting biotites. Neues Jahrbuch für Mineralogie Abhandlungen, 153, 147–161.

——— (1986b) Muscovite solid solutions in the system K_2O-MgO-FeO-Al_2O_3-SiO_2-H_2O: An experimental study at 2 kbar P_{H_2O} and comparison with natural Li-free white micas. Mineralogical Magazine, 50, 257–266.

——— (1986c) Evolution of the miscibility gap between muscovite and biotite solid solutions with increasing lithium content: An experimental study in the system K_2O-Li_2O-MgO-FeO-Al_2O_3-SiO_2-H_2O-HF at 600 °C, 2 kbar P_{H_2O}: Comparison with natural lithium micas. Mineralogical Magazine, 50, 641–651.

Munoz, J.L., and Swenson, A. (1981) Chloride-hydroxyl exchange in biotite and estimation of relative HCl/HF activities in hydrothermal fluids. Economic Geology, 76, 2212–2221.

Puziewicz, J. (1990) Post-magmatic origin of almandine-spessartine garnet in the Strzeblów alaskite (Stregom-Sobótka granite massif, SW Poland). Neues Jahrbuch für Mineralogie Monatshefte, 168–175.

Rock-Color Chart Committee (1980) Rock-color chart. Geological Society of America, Boulder, Colorado.

Russell, G.S., Speer, J.A., and Russell, C.W. (1985) The Portsmouth granite, a 263 Ma postmetamorphic biotite granite beneath the Atlantic Coastal Plain, Suffolk, Virginia. Southeastern Geology, 26, 81–93.

Snow, E., and Kidman, S. (1990) Experiments on melting in the granite system: Water absent, fluorine enriched. Eos, 71, 649.

Solberg, T.N., and Speer, J.A. (1982) QALL, a 16-element analytical scheme for efficient petrologic work on an automated ARL-SEMQ microprobe: Application to mica reference samples. In K.F.J. Heinrich, Ed., Microbeam analysis—1982, p. 422–426. San Francisco Press, San Francisco.

Speer, J.A. (1981) Petrology of cordierite- and almandine + cordierite-bearing biotite granitoid plutons of the southern Appalachian Piedmont, USA. Canadian Mineralogist, 19, 35–46.

——— (1982) Descriptions of granitoid rocks associated with two gravity minima in Aiken and Barnwell Counties, South Carolina. South Carolina Geology, 26, 15–24.

——— (1984) Igneous micas. In Mineralogical Society of America Reviews in Mineralogy, 13, 299–349.

——— (1987) Evolution of magmatic AFM mineral assemblages in granitoid rocks: The hornblende + melt = biotite reaction in the Liberty Hill pluton, South Carolina. American Mineralogist, 72, 863–878.

Speer, J.A., and Becker, S.W. (1990) The Cuffytown Creek pluton, Edgefield and McCormick Counties, South Carolina: A highly fractionated alkali-feldspar granite. South Carolina Geology, 33, 1–17.

Speer, J.A., Becker, S.W., and Farrar, S.S. (1980) Field relations and petrology of the postmetamorphic, coarse-grained granites and associated rocks in the southern Appalachian Piedmont. VPI&SU Memoir 2, 137–148.

Speer, J.A., van Gelder Brauer, S., and McSween, H.Y., Jr. (1986) The Bald Rock granitic pluton, South Carolina: Petrography and internal fabric. South Carolina Geology, 30, 1–17.

Thompson, A.B., and Tracy, R.J. (1979) Model systems for anatexis of pelitic rocks II. Facies series melting and reactions in the system CaO-$KAlO_2$-$NaAlO_2$-Al_2O_3-SiO_2-H_2O. Contributions to Mineralogy and Petrology, 70, 429–438.

Velde, B. (1965) Phengite micas: Synthesis, stability and natural occurrence. American Journal of Science, 263, 886–913.

Webster, J.D. (1990) Partitioning of F between H_2O and CO_2 fluids and topaz rhyolite melt. Contributions to Mineralogy and Petrology, 104, 424–438.

Wones, D.R., and Eugster, H.P. (1965) Stability of biotite: Experiment, theory, and applications. American Mineralogist, 50, 1228–1272.

Woodsworth, G.J. (1977) Homogenization of zoned garnets from pelitic schists. Canadian Mineralogist, 15, 230–242.

Yardley, B.W.D. (1977) An empirical study of diffusion in garnet. American Mineralogist, 62, 793–800.

Zen, E-an (1988) Phase relations of peraluminous granitic rocks and their petrogenetic implications. Annual Reviews of Earth and Planetary Sciences, 16, 21–51.